Applied Surface Science 702 (2025) 163315

Contents lists available at ScienceDirect

Applied Surface Science

journal homepage: www.elsevier.com/locate/apsusc

Short Communication

Carbon quantum dots implanted sulfonated 2D-MoS_2 for hydrogen evolution

Akash Sarkar [a], Gayathry Ganesh [b], Ummiya Qamar [a], Vivek Kumar Singh [a,1], Ruchi Sharma [a], Ankur Srivastava [c], Gunasekaran Venugopal [c], Rajan Jose [b,d], Santanu Das [a,*]

[a] Department of Ceramic Engineering, Indian Institute of Technology (BHU), Varanasi Uttar Pradesh 221005, India
[b] Faculty of Industrial Sciences and Technology, Universiti Malaysia Pahang Al-Sultan Abdullah, 26300 Kuantan, Pahang, Malaysia
[c] Department of Materials Science, School of Technology, Central University of Tamil Nadu, Thiruvarur 610005 Tamil Nadu, India
[d] Battery Research Center of Green Energy, Ming Chi University of Technology, 24301 New Taipei City, Taiwan

A B S T R A C T

We report the enhancement of electrocatalytic activity in sulfonate ($-SO_3H$) group functionalized two-dimensional molybdenum disulfide (2D-s-MoS_2) nanosheets for their use in hydrogen evolution reaction (HER). These as-developed nanosheets have been decorated with sustainable biomass-derived carbon quantum dots (CQDs) via a sonochemical method, creating a s-MoS_2-CQD composite material. This innovative composite demonstrates significantly improved electrocatalytic performance for the hydrogen evolution reaction (HER) via water splitting. In particular, incorporating CQDs on 2D-s-MoS_2 overcomes many limitations, as observed in pristine 2D-MoS_2 and 2D-s-MoS_2, especially regarding low electrical conductivity and restricted electrocatalytic activity on the basal plane. Incorporating CQDs enhances electron transfer efficiency, increases the availability of active sites, and enhances overall conductivity. As a result, the s-MoS_2-CQD achieves remarkable HER performance, featuring a lower overpotential of ~ 273 mV and a reduced Tafel slope of 67 mV/dec compared to s-MoS_2. These enhancements signify faster reaction kinetics, accelerated H^* adsorption–desorption, and greater catalytic efficiency. Furthermore, using sustainably synthesized CQDs positions this approach as a cost-effective, scalable, and environmentally friendly alternative to traditional noble-metal catalysts. This research highlights the potential of functionalized two-dimensional materials, such as s-MoS_2, implanted with zero-dimensional materials, such as CQDs, to advance sustainable hydrogen production technologies, thereby contributing to the global shift towards clean energy solutions.

1. Introduction

The increasing global demand for energy increased the need for sustainable alternatives to replace conventional power sources like fossil fuels. These energy production sources contribute to environmental issues, including global warming and climate change [1,2]. In recent years, carbon emissions have increased significantly due to the high demand for energy from fuels for vehicles and electricity for industries [3,4]. Hydrogen is crucial for addressing the shortages of solar and wind energy, as it serves as a versatile fuel, energy carrier, and catalyst for producing compounds like methanol and ammonia [5,6]. Moreover, the high energy yield (approximately 122 kJ) of hydrogen, environmental friendliness, and non-toxic by-products generated during combustion make hydrogen a viable renewable energy source [3,7]. The sustainability of hydrogen generation is crucial for transitioning to a low-carbon future and addressing the pressing challenges of climate change [8]. Hydrogen has great potential as a clean energy carrier, but its environmental benefits heavily rely on the methods used for its production. Traditional hydrogen production techniques, such as steam methane reforming, depend significantly on fossil fuels and release substantial amounts of carbon dioxide which undermines the goal of decarbonization [9,10]. Therefore, it is imperative to develop sustainable hydrogen production technologies, such as water electrolysis powered by renewable energy sources like solar, wind, and hydropower, that can produce zero emissions. These technologies also help to connect renewable energy supply and demand by acting as fuel and an energy storage medium [11–13]. Water electrolysis is a clean, effective, and sustainable method for replacing fossil fuels. This process uses water as the only starting molecule and produces water as a by-product in the hydrogen economy cycle, where burning hydrogen (H_2) releases energy while simultaneously generating water [14]. Noble metals such as Platinum (Pt) show exceptional electrocatalytic activities for Hydrogen generation due to high hydrogen bonding energy (HBE) and low hydrogen desorption energy (HDE) which makes it an excellent choice for the hydrogen evolution reaction (HER) [14], however due to the high cost and less availability, finding alternatives with the same order

* Corresponding author.
E-mail address: santanudas.cer@iitbhu.ac.in (S. Das).
[1] Present Address: Department of Chemistry, Center for Nanoscience and Nanotechnology, Hebrew University of Jerusalem, 91904, Jerusalem, Israel.

https://doi.org/10.1016/j.apsusc.2025.163315
Received 9 February 2025; Received in revised form 27 March 2025; Accepted 18 April 2025
Available online 20 April 2025

of properties (cost-effective, stable, low-overpotential) are required for large scale hydrogen generation. Transition metal dichalcogenides (TMDs), especially molybdenum disulfide (MoS_2), have gained significant attention as promising catalysts for hydrogen evolution reactions [15–17]; specifically, 2D-MoS_2 possesses several highly desirable properties, including a high surface area and exceptional stability in acidic conditions [18,19]. However, the catalytic performance of pristine MoS_2 has some limitations, such as low electrical conductivity and low catalytically active basal planes for HER [20–23]. These restricted availabilities of active sites reduce the overall catalytic efficiency of the material. Intense research for enhancing the electrocatalytic activities of MoS_2 basal planes includes ion irradiation [24], phase transformation in 1T-MoS_2 (metallic state) [25–27], introducing defects [28,28,29], vertically grown structure [30,31], functionalization of MoS_2 [18,32–34] etc. In our previous work, we have reported the benefits of functionalizing MoS_2 nanosheets by sulfonic group (SO_3H^-) [33]. The incorporation of the SO_3H^- group into MoS_2 (s-MoS_2) enhances its electrocatalytic activity, demonstrating improved performance compared to pristine MoS_2. However, despite this enhancement, the presence of the SO_3H^- group reduces electrical conductivity, thereby increasing electrical resistivity. Specifically, in s-MoS_2, the intercalation of SO_3H^- groups between the MoS_2 layers disrupts the basal plane, introduces defects, and hinders electron transfer, limiting further improvements in electrocatalytic properties. To address this challenge, integrating conducting nanoparticles, such as carbon quantum dots (CQDs), presents a promising strategy to enhance both the electrocatalytic activity and electronic conductivity of s-MoS_2. Previous studies have shown that CQD-integrated MoS_2 exhibits lower charge transfer resistance compared to pristine MoS_2, leading to accelerated charge transfer kinetics. This improvement plays a crucial role in various electrochemical applications of s-MoS_2, where enhanced conductivity facilitates rapid electron movement during redox reactions, ultimately boosting overall electrochemical performance [35].

Carbon quantum dots (CQDs) are tiny structures that have applications in various fields, including biomedicine, optoelectronics, catalysis, energy storage, and sensors [36–39]. CQDs are synthesized from a variety of precursors which include synthetic materials like small molecules, polymers, and biomass. The biomass-derived CQDs are of great interest because they are cost-effective (due to minimal processing and usage of renewable precursors), sustainable, flexible in different pH environments, and naturally functionalised, which eliminates the requirement of post-functionalisation [37,39,40]. The presence of intrinsic functionalities such as hydroxyl, carboxyl and amino are highly beneficial for improving the surface wettability and improving the HER activity. Further, the functional groups on the surface of CQDs enable them to readily combine with other compounds like MoS_2 and boost their catalytic activity [41,42]. Studies indicate that integrating CQDs with MoS_2 could enhance electron transfer from the conjugated carbon core to the MoS_2 layers, thereby improving the in-plane electrical conductivity. Additionally, CQD integration increases the concentration of S_2^{2-} and S^{2-} species, which facilitates hydrogen adsorption on the MoS_2 surface, further enhancing its catalytic performance [41,43]. Combined with the higher surface area of CQDs, the HER activity of the composite could be boosted.

This research presents to significantly enhance the catalytic performance of sulfonated MoS_2 (s-MoS_2) nanosheets for hydrogen evolution by incorporating carbon quantum dots (CQDs) through a sustainable sonochemical approach. Sulfonation improves electron transfer, while CQD integration enhances conductivity and increases active catalytic sites, addressing the limited electrochemical catalytic activity of pristine MoS_2 basal planes. The resulting s-MoS_2-CQD composite demonstrates outstanding HER performance, exhibiting a lower overpotential and Tafel slope, indicative of accelerated reaction kinetics and reduced charge transfer resistance. By utilizing CQDs sustainably synthesized from biomass, this work offers a cost-effective and scalable alternative to noble-metal catalysts, contributing to sustainable hydrogen production and advancing clean energy solutions. MoS_2 nanosheets were synthesized via a one-pot hydrothermal method, followed by CQD implantation using a sonochemical process. Structural and compositional analyses were conducted using X-ray diffraction (XRD), transmission electron microscopy (TEM), Fourier-transform infrared spectroscopy (FTIR), X-ray photoelectron spectroscopy (XPS), and Raman spectroscopy. Electrochemical studies further confirmed the enhanced catalytic kinetics for hydrogen generation.

2. Results and Discussion

The synthesis and characterizations of s-MoS_2-CQD and its electrode preparation is demonstrated in the Experimental section S1, Fig. S1 and Fig. S2 (supporting information). Fig. 1a shows the XPS spectrum of two characteristic peaks at binding energies of approximately 229.68 eV ($3d_{5/2}$) and 232.78 eV ($3d_{3/2}$) corresponding to Mo 3d thereby confirming the Mo^{4+} oxidation state of molybdenum [44]. Additionally, a small peak for the S 2s is visible around 226.88 eV. Fig. 1b presents the sulfur 2p peaks of s-MoS_2 at 161.28 eV and 162.28 eV, corresponding to S $2p_{3/2}$ and S $2p_{1/2}$, respectively, confirming the elemental composition of MoS_2 [33,44]. A similar peak profile is observed in the XPS spectrum of s-MoS_2-CQD (as shown in Fig. 1b), indicating that the oxidation state of Mo remains unchanged even after CQD implantation onto s-MoS_2 nanosheets. However, a peak shift of approximately 0.9 eV towards lower binding energy is detected, likely due to localized defects introduced during CQD implantation during the sonochemical process [45]. The XPS spectra (Fig. 1c-d) at a binding energy of approximately 168.5 eV confirm the successful functionalization of sulfonic groups on the MoS_2 surface, verifying the formation of s-MoS_2. This functionalization enhances electronic properties by promoting surface charge transfer across the s-MoS_2 nanosheets. [33] Such functionalizations can further be correlated to the increased intensity of the S^{2-} peak, which suggests improved H^+ adsorption [43]. The XPS spectrum of C 1s of s-MoS_2- CQD is also analysed in Fig. S3 (Section S2) of the supporting information identifying three distinct peaks observed at 284.18 eV, 285.58 eV and 287.69 eV corresponding to –C–C/C=C, –C–O, and –C=O bonds, respectively. These peaks are prominent in CQD, indicating no chemical bonding with 2D-MoS_2[46].

Fig. 2 illustrates the HR-TEM and selected area electron diffraction (SAED) images, demonstrating the structural characteristics of s-MoS_2 and s-MoS_2-CQDs. The fringes in HR-TEM images, Fig. 2a and 2b, show the few layers with an interlayer spacing of 0.63 nm representing the (002) plane of s-MoS_2 nanosheets. The TEM image and SAED pattern of s-MoS_2 are given in the of the manuscript Fig. S4, (Section S2, supporting information). Fig. 2c illustrates CQDs securely embedded on the s-MoS_2 surface, with the (010) plane highlighting the interaction between CQDs and s-MoS_2. Fig. 2d depicts three diffraction rings appear in the SAED pattern showing (010), (013), and (110) planes corresponding to d spacings of 2.77, 2.28, and 1.58, respectively, confirming undisrupted crystallinity of s-MoS_2 after the CQD implantation.

Fig. 3a shows the XRD data with peak positions are 14°, 33.24°, 39.50°, 48.86°, 58.88° and 69.50° corresponding to planes (002), (010), (013), (105), (110), and (021), respectively. The XRD data presents hexagonal phase of 2D-MoS_2 nanosheets, in after matching the peak positions with the JCPDS card no. 98–001-8125 [47]. Fig. 3b shows comparative Raman spectra of s-MoS_2 and s-MoS_2-CQD demonstrating the in-plane (E_{2g}) and out-plane (A_{1g}) vibrations are at 376 cm^{-1} and 406 cm^{-1}, respectively, verifying the formation of multilayed two-dimensional, s-MoS_2 nanosheets. For s-MoS_2-CQD, the characteristic E_{2g} & A_{1g} peak positions were found at 376 cm^{-1} and 400 cm^{-1}, respectively[48]. However, characteristic G-band (1380 cm^{-1}) and D-band (1584 cm^{-1}) of carbon in the Raman spectrum of s-MoS_2-CQD (Fig. 3b) specifically suggested the successful implantation of CQDs in s-MoS_2 nanosheets [49]. The G-band represents the association of the CQD with graphitization in sp^2 hybridization, whereas the D-band is due to the defects or functionalization in sp^3 hybridization [50].

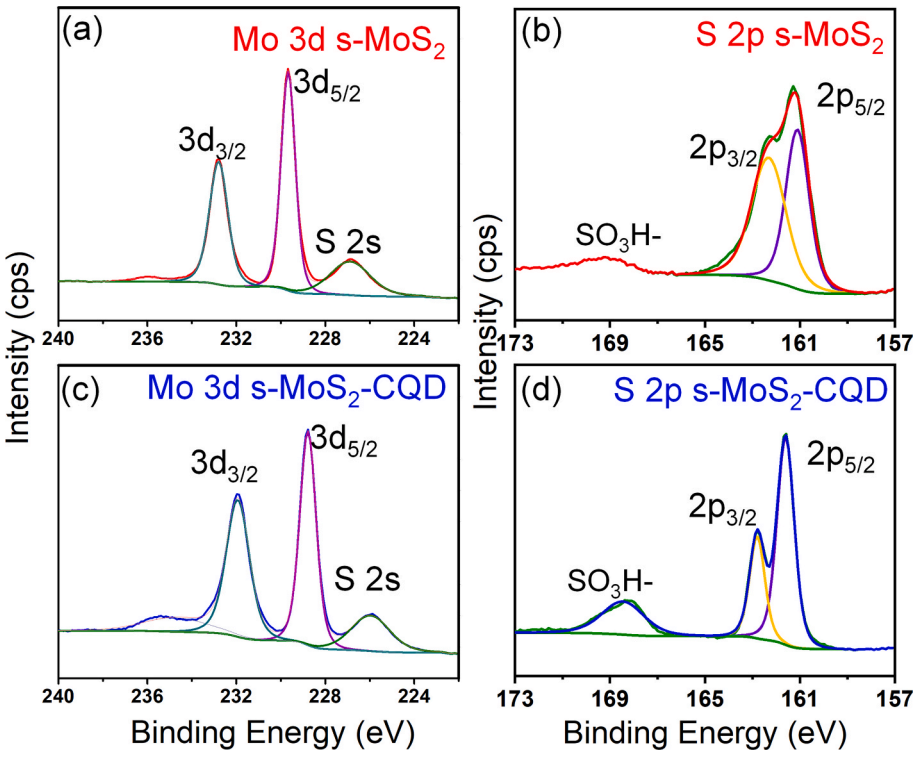

Fig. 1. XPS spectrum of (a) Mo 3d, (b) S 2p for s-MoS_2; and (c) Mo 3d, (d) S 2p for s-MoS_2-CQD respectively.

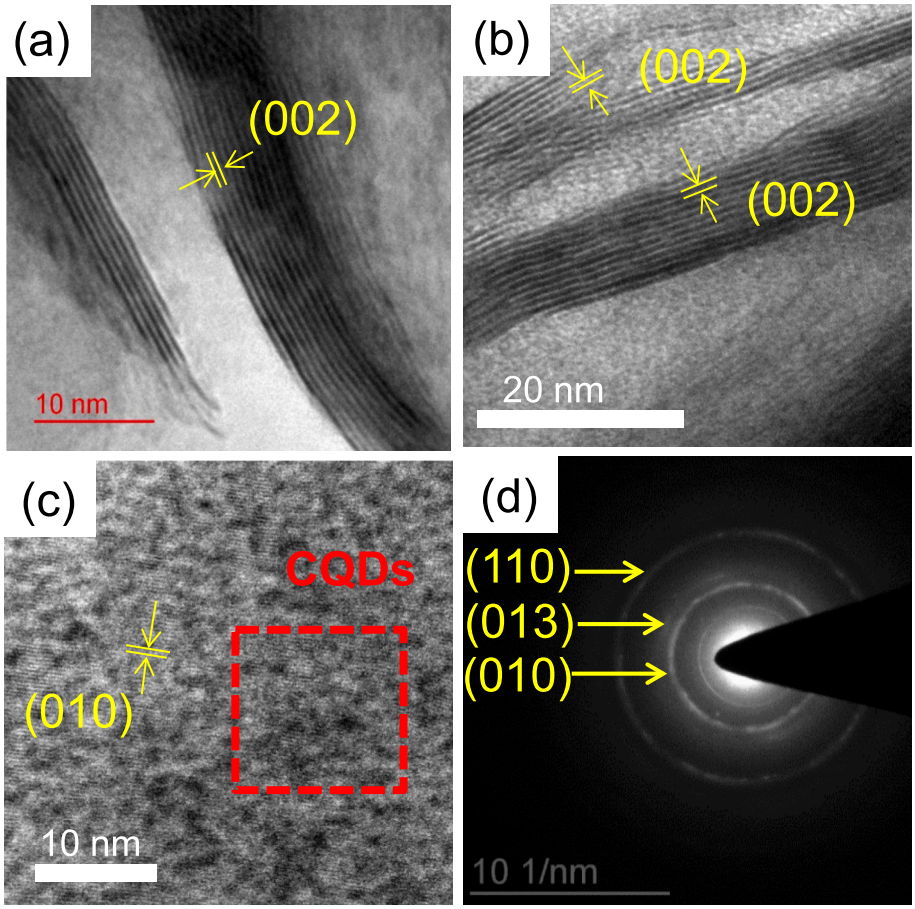

Fig. 2. HRTEM images of (a) s-MoS_2, (b) s-MoS_2-CQD interlayer spacing, (c) CQD implanted on s-MoS_2 nanosheets and (d) SAED pattern of s-MoS_2-CQD nanosheets.

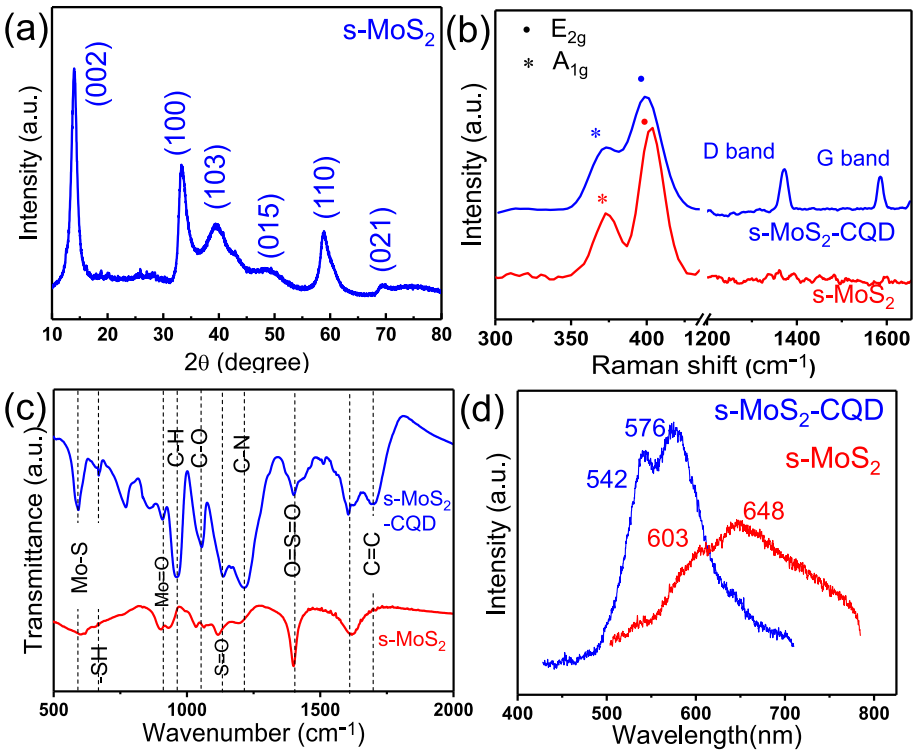

Fig. 3. (a) XRD pattern of s-MoS_2. Comparative (b) Raman spectra, (c) FTIR spectrum and (d) PL spectra of s-MoS_2 and s-MoS_2-CQD.

Additionally, the homogeneous implantation of CQD in MoS_2 nanosheets was further confirmed by acquiring the Raman mapping, as shown in Fig. S5 (Section S2, supporting information), which shows intact G and D bands at their respective wavenumbers.

FTIR spectroscopy was used to evaluate the functional group and the formation in s-MoS_2 and s-MoS_2-CQD, as shown in Fig. 3c. The transmittance band at 590 cm^{-1} is attributed to MoS_2 [51], and 1690 cm^{-1} is typically associated with carbon, which arises from the stretching of C=C bonds, which in turn indicates the presence of carbon in the composite material (s-MoS_2-CQD) [52]. The strong peak extending in the range of 1000–1350 cm^{-1} contains the contribution from C-O, C-N and S=O stretching mode.[33,39,52] The band around 663 cm^{-1} possibly arises due to the stretching vibration of −SH [53]. Due to the presence of minor impurities in the samples, some additional peaks (around 760 cm^{-1} and 1622 cm^{-1}) were also observed. Further, PL spectroscopy was performed to compare the optical properties of s-MoS_2 and s-MoS_2-CQD. In Fig. 3d, the B-exciton (603 nm) and A-exciton (648 nm) can be identified for MoS_2 [54] where the significant blue shift in the PL peak positions (542 nm and 576 nm respectively) was also noticeable for s-MoS_2-CQD which might be the result of increased

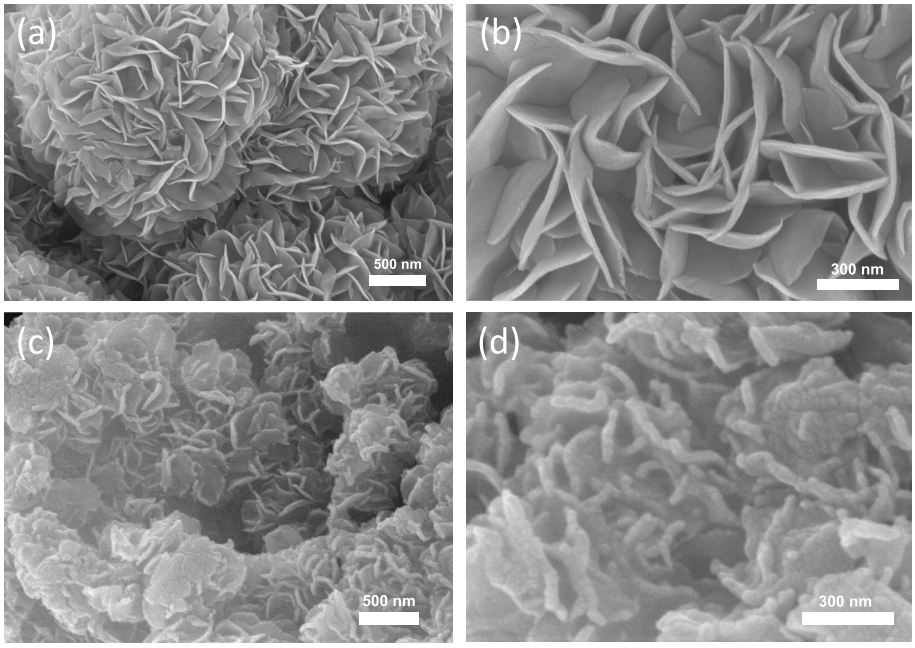

Fig. 4. SEM images of (a), (b) s-MoS_2 and (c), (d) s-MoS_2-CQD nanocomposite.

bandgap after the interaction of s-MoS_2 and CQD, compared to pristine s-MoS_2. The implantation of CQDs onto s-MoS_2 leads to a substantial increase in the effective band gap of the composite material that can further be tuned by altering the composite concentration in solution [55,56]. This enhancement is a direct result of the unique electronic interactions at the interface between CQDs and s-MoS_2, which effectively altering the radiative recombination dynamics and promote efficient charge seperation. Consequently, the effective band gap of the s-MoS_2-CQD system is markedly increased, optimizing its performance across UV to NIR wavelengths. The incorporation of CQDs into s-MoS_2 improves the system's electronic properties, enhancing charge separation and transport efficiency [57].

The surface morphology of the as-synthesized s-MoS_2 is displayed in Fig. 4a & b. It was observed from the SEM micrographs that the nanosheets were comprised of large surface areas stacked on each other, depicting sharp edges and organized in a flower-like pattern. Fig. 4c & d shows the surface of CQD-implanted s-MoS_2 morphology seems to change as the CQDs were implanted on MoS_2 nanosheets by the sonochemical method, with the nanosheets becoming less densely packed and more disordered. Although the high-frequency sonication process does not entirely break the layered structure of MoS_2, it creates additional surfaces and disordered thick edges, which increase the surface area, resulting in high electrocatalytic activity for hydrogen evolution.

All the electrochemical investigations were carried out for both s-MoS_2 and s-MoS_2-CQD to evaluate their effectiveness in the photocatalytic HER reactions. Fig. 5a shows an increase in the current density of s-MoS_2-CQD samples, found to be 216 mA/cm^2 as compared to s-MoS_2 that exhibit a current density of 173 mA/cm^2, in accordance with the overpotentials observed to be 350 mV and 273 mV for s-MoS_2 and s-MoS_2-CQD, respectively. The Tafel slope reduced to 67 mV/decade in s-MoS_2-CQD, which was found to be 76 mV/decade, slightly higher in s-MoS_2, as is shown in Fig. 5b. Fig. 5c & 5d plots the CV curves at different scan rates for both s-MoS_2 and s-MoS_2-CQD samples. It is evident from the CV curves that when CQDs were anchored onto the layers of s-MoS_2, the electrochemical surface area increased.

Fig. 5e depicts a typical EIS plot, giving R_{ct} values of 1.45 Ω and 2.20 Ω for s-MoS_2-CQD and s-MoS_2, respectively, satisfying the increase in current density shown in Fig. 5a. The lowering of R_{ct} indicates efficient electron transfer. Fig. 5f gives the C_{dl} plot, showing the double-layer capacitance for both s-MoS_2 and s-MoS_2-CQD. The fitting data shows that the addition of CQDs nearly doubles the C_{dl} value, indicating that the CQDs contribute to increasing the electrochemical surface area for catalytic activities. The stability was evaluated through chronoamperometry, as is shown in Fig. S6 (supporting information), where the prepared s-MoS_2-CQD showed stability for a period of ~11 h. The comparative electrochemical results for s-MoS_2 and s-MoS_2-CQD is

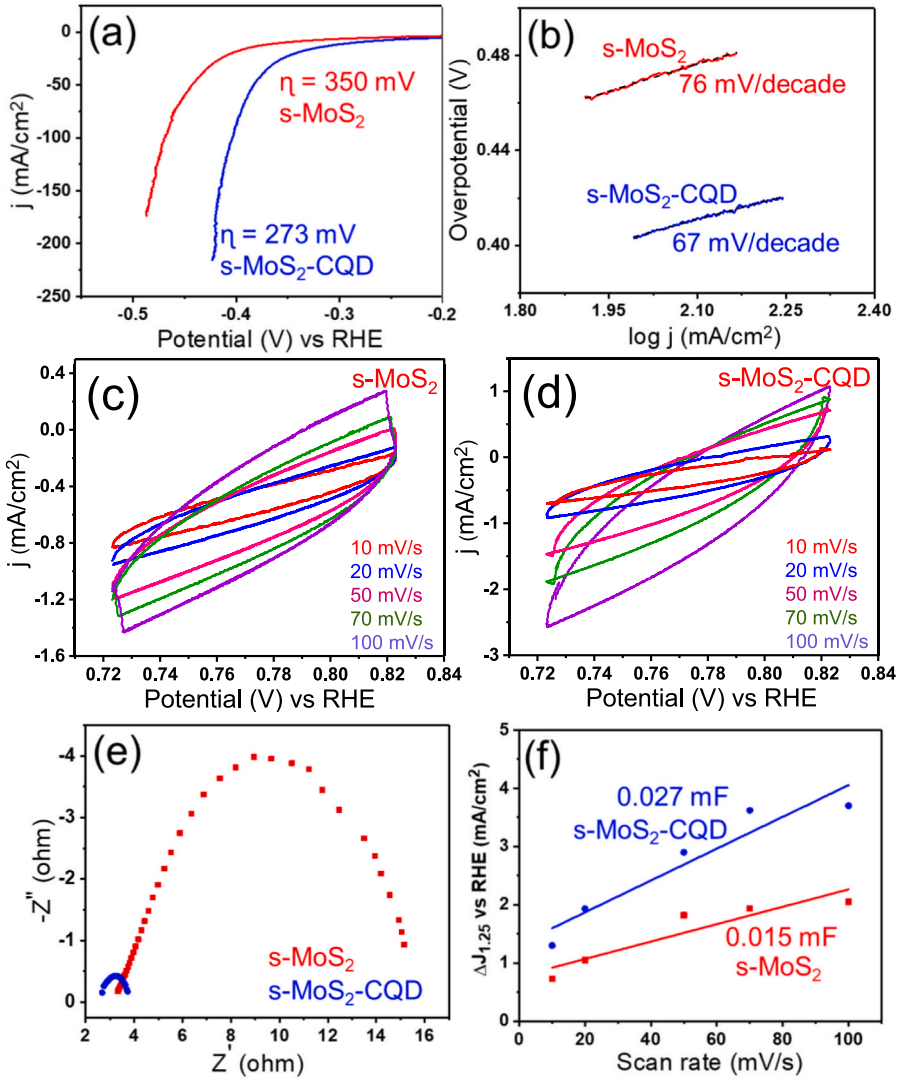

Fig. 5. (a) LSV; (b) Tafel plots; (c and d) CV; (e) EIS; and (f) C_{dl} of s-MoS_2 and s-MoS_2-CQD.

shown in Table 1.

Overall, as highly efficient electron donors, carbon quantum dots (CQDs) induce surface charge redistribution on MoS_2, establishing a proton-favorable gradient that enhances adsorption. This process accelerates proton migration from CQDs to sulfonated MoS_2 (s-MoS_2), significantly improving the hydrogen evolution reaction (HER) kinetics. The extensive π-conjugation in CQDs critically facilitates electron injection into s-MoS_2, effectively suppressing S^{4+} sites while substantially enriching catalytically active S_2^{2-} and S^{2-} species. Such electronic modulation creates sulfur vacancies in s-MoS_2, which further promotes hydrogen adsorption through exposed unsaturated sulfur sites. Furthermore, the restructured electronic configuration increases the density of states near the Fermi level, dramatically enhancing charge transport efficiency during electrocatalysis. Coupled with their large electrochemically active surface area and multifunctional groups, CQDs impart superior conductivity to the composite system, effectively overcoming MoS_2's intrinsic charge transport limitations. This work not only demonstrates a high-performance HER catalyst but also establishes a design framework for developing diverse 0D-2D hybrid architectures with synergistic properties for advanced electrocatalytic applications.

3. Conclusion

This study reports enhancements in the catalytic efficiency of s-MoS_2 by implanting biomass derived carbon quantum dots (CQDs) on MoS_2 nanosheets functionalized with a sulfonic group (−SO_3H). While pristine MoS_2 exhibits good stability and surface area, its limited electrical conductivity and activity on the basal plane restrict its catalytic performance. Functionalizing MoS_2 with sulfonic groups (SO_3H^-) improves electron transfer, and the addition of CQDs further enhances conductivity, electrochemical surface area, and active sites through a sonochemical method. The CQDs introduced an improvement in s-MoS_2 by altering its morphology such that it has a higher surface area and by improving the catalytic activity of sulfur-containing edge groups, mediated functional moieties on the surface of CQDs. The electrochemical analysis thus demonstrated improved HER performance, with the s-MoS_2-CQD composite showing a lower overpotential of 273 mV compared to s-MoS_2. Furthermore, it exhibited a reduced Tafel slope of 67 mV/decade, indicating faster reaction kinetics. The CQD-implanted composite also showed enhanced double-layer capacitance and reduced charge transfer resistance (R_{ct}), highlighting its potential as a cost-effective and durable catalyst for sustainable hydrogen production. Additionally, the study reveals the increased band gap of the MoS_2 by implanting CQDs onto its surface, which makes a valuable addition to the electronic property of s-MoS_2 nanosheets.

CRediT authorship contribution statement

Akash Sarkar: Writing – original draft, Visualization, Software, Formal analysis, Data curation. **Gayathry Ganesh:** Writing – original draft, Resources, Methodology, Formal analysis, Data curation. **Ummiya Qamar:** Writing – original draft, Validation, Software, Methodology, Formal analysis, Data curation. **Vivek Kumar Singh:** Writing – review & editing, Software, Resources, Investigation, Formal analysis. **Ruchi Sharma:** Writing – original draft, Software, Formal analysis, Data curation. **Ankur Srivastava:** Writing – original draft, Validation, Methodology, Data curation. **Gunasekaran Venugopal:** Writing – review & editing, Resources, Investigation, Formal analysis. **Rajan Jose:** Writing – review & editing, Validation, Supervision, Methodology, Investigation. **Santanu Das:** Methodology.

Declaration of competing interest

The authors declare the following financial interests/personal relationships which may be considered as potential competing interests: [Santanu Das reports financial support was provided by Indian Institute of Technology (BHU) Varanasi, DRDO AND SERB. Santanu Das reports a relationship with Indian Institute of Technology (BHU) Varanasi that includes: employment. Not Applicable If there are other authors, they declare that they have no known competing financial interests or personal relationships that could have appeared to influence the work reported in this paper.].

Table 1
Lists the comparative electrochemical parameters for the s-MoS_2 and s-MoS_2-CQD.

Samples	η_{10} (mV)	Tafel slope (mV/dec)	C_{dl} (mF)
s-MoS_2	350	76	0.015
s-MoS_2-CQD	273	67	0.027

Acknowledgements

Dr Santanu Das (SD) gratefully acknowledges the SERB Core Research grant (Grant no: CRG/2022/003204) and DRDO ERIP grant (Grant no: ERIP/ER/202310001/M/01/1849) for providing financial support for this work.

Appendix A. Supplementary data

Supplementary data to this article can be found online at https://doi.org/10.1016/j.apsusc.2025.163315.

Data availability

Data will be made available on request.

References

[1] T.Z. Ang, M. Salem, M. Kamarol, H.S. Das, M.A. Nazari, N. Prabaharan, A comprehensive study of renewable energy sources: Classifications, challenges and suggestions, Energy Strateg. Rev. 43 (2022) 100939, https://doi.org/10.1016/j.esr.2022.100939.
[2] S.K. Dash, S. Chakraborty, D. Elangovan, A Brief Review of Hydrogen Production Methods and Their Challenges, Energies 16 (2023), https://doi.org/10.3390/en16031141.
[3] M.K. Sarmah, T.P. Singh, P. Kalita, A. Dewan, Sustainable hydrogen generation and storage - a review, RSC Adv. 13 (2023) 25253–25275, https://doi.org/10.1039/d3ra04148d.
[4] P.J. Megia, A.J. Vizcaino, J.A. Calles, A. Carrero, Hydrogen Production Technologies: From Fossil Fuels toward Renewable Sources, A Mini Review, Energy and Fuels 35 (2021) 16403–16415, https://doi.org/10.1021/acs.energyfuels.1c02501.
[5] M. Shi, X. Meng, Photothermal catalysis: From principles to applications, Int. J. Hydrogen Energy 48 (2023) 34659–34676, https://doi.org/10.1016/j.ijhydene.2023.05.253.
[6] L. Petrescu, S.-C. Galusnyak, D.-A. Chisalita, C.-C. Cormos, Modelling and Simulation of Methanol Production and Conversion into Various Chemical Intermediates and Products, in: S. Pierucci, F. Manenti, G.L. Bozzano, D.B.T.-C.A.C. E. Manca (Eds.), 30 Eur. Symp. Comput. Aided Process Eng., Elsevier, 2020: pp. 553–558. Doi: Doi: 10.1016/B978-0-12-823377-1.50093-8.
[7] G. AlZohbi, An Overview of Hydrogen Energy Generation, ChemEngineering 8 (2024), https://doi.org/10.3390/chemengineering8010017.
[8] E.B. Agyekum, C. Nutakor, A.M. Agwa, S. Kamel, A Critical Review of Renewable Hydrogen Production Methods: Factors Affecting Their Scale-Up and Its Role in Future Energy Generation, Membranes (basel). 12 (2022), https://doi.org/10.3390/membranes12020173.
[9] M. Kayfeci, A. Keçebaş, M. Bayat, Chapter 3 - Hydrogen production, in: F. Calise, M.D. D'Accadia, M. Santarelli, A. Lanzini, D.B.T.-S.H.P. Ferrero (Eds.), Academic Press, 2019: pp. 45–83. Doi: Doi: 10.1016/B978-0-12-814853-2.00003-5.
[10] V. Singh, D. Das, Chapter 3 - Potential of Hydrogen Production From Biomass, in: P.E.V.B.T.-S. and E. of H.-B.E.T. de Miranda (Ed.), Academic Press, 2019: pp. 123–164. Doi: Doi: 10.1016/B978-0-12-814251-6.00003-4.
[11] A. Gupta, B. Likozar, R. Jana, W.C. Chanu, M.K. Singh, A review of hydrogen production processes by photocatalytic water splitting – From atomistic catalysis design to optimal reactor engineering, Int. J. Hydrogen Energy 47 (2022) 33282–33307, https://doi.org/10.1016/j.ijhydene.2022.07.210.
[12] X. Li, L. Zhao, J. Yu, X. Liu, X. Zhang, H. Liu, W. Zhou, Water Splitting: From Electrode to Green Energy System, Nano-Micro Lett. 12 (2020) 1–29, https://doi.org/10.1007/s40820-020-00469-3.

[13] S. Roy, U. Qamar, A.A. Sasikala Devi, S. Das, Recent progresses on Janus electrocatalysts for water electrolysis: A critical review, APL Energy 2 (2024). Doi: 10.1063/5.0176450.

[14] J. Zhu, L. Hu, P. Zhao, L.Y.S. Lee, K.Y. Wong, Recent Advances in Electrocatalytic Hydrogen Evolution Using Nanoparticles, Chem. Rev. 120 (2020) 851–918, https://doi.org/10.1021/acs.chemrev.9b00248.

[15] J. Deng, W. Yuan, P. Ren, Y. Wang, D. Deng, Z. Zhang, X. Bao, High-performance hydrogen evolution electrocatalysis by layer-controlled MoS2 nanosheets, RSC Adv. 4 (2014) 34733–34738, https://doi.org/10.1039/c4ra05614k.

[16] T. Manyepedza, J.M. Courtney, A. Snowden, C.R. Jones, N.V. Rees, Impact Electrochemistry of MoS2: Electrocatalysis and Hydrogen Generation at Low Overpotentials, J. Phys. Chem. C 126 (2022) 17942–17951, https://doi.org/10.1021/acs.jpcc.2c06055.

[17] S. Jayabal, G. Saranya, J. Wu, Y. Liu, D. Geng, X. Meng, Understanding the high-electrocatalytic performance of two-dimensional MoS2 nanosheets and their composite materials, J. Mater. Chem. A 5 (2017) 24540–24563, https://doi.org/10.1039/c7ta08327k.

[18] B. Lai, S.C. Singh, J.K. Bindra, C.S. Saraj, A. Shukla, T.P. Yadav, W. Wu, S. A. McGill, N.S. Dalal, A. Srivastava, C. Guo, Hydrogen evolution reaction from bare and surface-functionalized few-layered MoS2 nanosheets in acidic and alkaline electrolytes, Mater. Today Chem. 14 (2019), https://doi.org/10.1016/j.mtchem.2019.100207.

[19] N. Abidi, A. Bonduelle-Skrzypczak, S.N. Steinmann, How Stable Are 2H-MoS2Edges under Hydrogen Evolution Reaction Conditions? J. Phys. Chem. C 125 (2021) 17058–17067, https://doi.org/10.1021/acs.jpcc.1c04492.

[20] W. Li, G. Liu, J. Li, Y. Wang, L. Ricardez-Sandoval, Y. Zhang, Z. Zhang, Hydrogen evolution reaction mechanism on 2H-MoS2 electrocatalyst, Appl. Surf. Sci. 498 (2019) 143869, https://doi.org/10.1016/j.apsusc.2019.143869.

[21] H. Li, C. Tsai, A.L. Koh, L. Cai, A.W. Contryman, A.H. Fragapane, J. Zhao, H.S. Han, H.C. Manoharan, F. Abild-Pedersen, J.K. Nørskov, X. Zheng, Activating and optimizing MoS2 basal planes for hydrogen evolution through the formation of strained sulphur vacancies, Nat. Mater. 15 (2016) 48–53, https://doi.org/10.1038/nmat4465.

[22] U. Sharma, S. Karazhanov, N. Alonso-Vante, S. Das, Metallic-phase of MoS2 as potential electrocatalyst for hydrogen production via water splitting: A brief review, Curr. Opin. Electrochem. 35 (2022) 101067, https://doi.org/10.1016/j.coelec.2022.101067.

[23] U. Sharma, S. Karazhanov, R. Jose, S. Das, Plasmonic hot-electron assisted phase transformation in 2D-MoS2 for the hydrogen evolution reaction: current status and future prospects, J. Mater. Chem. A (2022) 8626–8655, https://doi.org/10.1039/d1ta10918a.

[24] J. Rmuš Mravik, I. Milanović, S. Milošević Govedarović, A. Mraković, E. Korneeva, I. Stojković Simatović, S. Kurko, Improvement of MoS2 electrocatalytic activity for hydrogen evolution reaction by ion irradiation, Int. J. Hydrogen Energy 48 (2023) 38676–38685, https://doi.org/10.1016/j.ijhydene.2023.06.178.

[25] U. Qamar, B. Mukherjee, A.A. Sasikala Devi, S. Das, Ordered Au3Cu Nanocrystals Induced Phase Transformation in 2D-MoS2 as SERS Substrate for Enhancing Molecular Detection, Cryst. Growth Des. 24 (2024) 5922–5933, https://doi.org/10.1021/acs.cgd.4c00170.

[26] U. Qamar, S. Roy, S. Kumar, B. Mukherjee, A.A.S. Devi, A. Goswami, P. Maiti, S. Das, Plasmonic Au3Cu Ordered Nanocrystals Induced Phase Transformation in 2D-MoS2 for Efficient Hydrogen Evolution, Adv. Funct. Mater. (2024) 2311943, https://doi.org/10.1002/adfm.202311943.

[27] S. Das, U. Sharma, B. Mukherjee, A.A. Sasikala Devi, J. Velusamy, Polygonal gold nanocrystal induced efficient phase transition in 2D-MoS2 for enhancing photo-electrocatalytic hydrogen generation, Nanotechnology 34 (2023), https://doi.org/10.1088/1361-6528/acade6.

[28] J. Xie, H. Zhang, S. Li, R. Wang, X. Sun, M. Zhou, J. Zhou, X.W. Lou, Y. Xie, Defect-rich MoS2 ultrathin nanosheets with additional active edge sites for enhanced electrocatalytic hydrogen evolution, Adv. Mater. 25 (2013) 5807–5813, https://doi.org/10.1002/adma.201302685.

[29] M.K. Kim, B. Lamichhane, B. Song, S. Kwon, B. Wang, S. Kattel, J.H. Lee, H. M. Jeong, Enhancing electrocatalytic hydrogen evolution of MoS2 enabled by electrochemical cation implantation for simultaneous surface-defect and phase engineering, Appl. Catal. B Environ. 352 (2024) 124037, https://doi.org/10.1016/j.apcatb.2024.124037.

[30] J. Joe, C. Bae, E. Kim, T.A. Ho, H. Yang, J.H. Park, H. Shin, Mixed-phase (2H and 1T) MoS2 catalyst for a highly efficient and stable si photocathode, Catalysts 8 (2018) 1–15, https://doi.org/10.3390/catal8120580.

[31] Z. Pan, X. Ji, Vertical growth of compact and large-area MoS(2) nanosheet arrays on Ti(3)C(2)T(x) for efficient bifunctional electrochemical energy storage and hydrogen evolution, J. Colloid Interface Sci. 650 (2023) 995–1002, https://doi.org/10.1016/j.jcis.2023.07.074.

[32] V.K. Singh, U. Gupta, B. Mukherjee, S. Chattopadhyay, S. Das, MoS2 Nanosheets on MoNi4/MoO2 Nanorods for Hydrogen Evolution, ACS Appl. Nano Mater. 4 (2021) 886–896, https://doi.org/10.1021/acsanm.0c03296.

[33] V.K. Singh, B. Mukherjee, S. Assa Aravindh, S. Das, Sulfonic acid (SO3H) functionalized two-dimensional MoS2 nanosheets for electrocatalytic hydrogen generation, Appl. Surf. Sci. 609 (2023) 155354, https://doi.org/10.1016/j.apsusc.2022.155354.

[34] S. Pak, J. Lim, J. Hong, S. Cha, Enhanced hydrogen evolution reaction in surface functionalized mos2 monolayers, Catalysts 11 (2021) 1–9, https://doi.org/10.3390/catal11010070.

[35] H. Teymourinia, S. Rtimi, M. Ghalkhani, A. Ramazani, T.M. Aminabhavi, Flower-like nanocomposite of carbon quantum dots, MoS2, and dendritic Ag-based Z-scheme type photocatalysts for effective tartrazine degradation, Chem. Eng. J. 473 (2023) 145239, https://doi.org/10.1016/j.cej.2023.145239.

[36] J. Liu, R. Li, B. Yang, Carbon Dots: A New Type of Carbon-Based Nanomaterial with Wide Applications, ACS Cent. Sci. 6 (2020) 2179–2195, https://doi.org/10.1021/acscentsci.0c01306.

[37] M. Fang, B. Wang, X. Qu, S. Li, J. Huang, J. Li, S. Lu, N. Zhou, State-of-the-art of biomass-derived carbon dots: Preparation, properties, and applications, Chinese Chem. Lett. 35 (2024) 108423, https://doi.org/10.1016/j.cclet.2023.108423.

[38] G. Ganesh, V. Sunil, J.K. Ling, U. Qamar, I.I. Misnon, B.K. Kuila, S. Das, C.C. Yang, R. Jose, Carbon dots as a sustainable electrolyte enhancer in aqueous alkaline electrochemical capacitors, J. Energy Storage 94 (2024) 112465, https://doi.org/10.1016/j.est.2024.112465.

[39] G. Ganesh, I. Izwan Misnon, R. Jose, Solvothermal synthesis of green fluorescent carbon dots from palm kernel shells, Mater. Today Proc. (2023), https://doi.org/10.1016/j.matpr.2023.02.332.

[40] A. Qureashi, A.H. Pandith, A. Bashir, L.A. Malik, Biomass-derived carbon quantum dots: a novel and sustainable fluorescent "ON–OFF–ON" sensor for ferric ions, Anal. Methods 13 (2021) 4756–4766, https://doi.org/10.1039/D1AY01112J.

[41] S. Zhao, C. Li, L. Wang, N. Liu, S. Qiao, B. Liu, H. Huang, Y. Liu, Z. Kang, Carbon quantum dots modified MoS2 with visible-light-induced high hydrogen evolution catalytic ability, Carbon N. Y. 99 (2016) 599–606, https://doi.org/10.1016/j.carbon.2015.12.088.

[42] L. Song, X. Zhang, S. Zhu, Y. Xu, Y. Wang, Hydrogen spillover effect enhanced by carbon quantum dots activated MoS2, Carbon N. Y. 199 (2022) 63–69, https://doi.org/10.1016/j.carbon.2022.07.071.

[43] B. Guo, K. Yu, H. Li, R. Qi, Y. Zhang, H. Song, Z. Tang, Z. Zhu, M. Chen, Coral-shaped MoS2 decorated with graphene quantum dots performing as a highly active electrocatalyst for hydrogen evolution reaction, ACS Appl. Mater. Interfaces 9 (2017) 3653–3660, https://doi.org/10.1021/acsami.6b14035.

[44] D. Ganta, S. Sinha, R.T. Haasch, 2-D Material Molybdenum Disulfide Analyzed by XPS, Surf. Sci. Spectra 21 (2014) 19–27, https://doi.org/10.1116/11.20140401.

[45] M.A. Baker, R. Gilmore, C. Lenardi, W. Gissler, XPS investigation of preferential sputtering of S from MoS2 and determination of MoSx stoichiometry from Mo and S peak positions, Appl. Surf. Sci. 150 (1999) 255–262, https://doi.org/10.1016/S0169-4332(99)00253-6.

[46] H. Teymourinia, S. Rtimi, M. Ghalkhani, A. Ramazani, T.M. Aminabhavi, Flower-like nanocomposite of carbon quantum dots, MoS2, and dendritic Ag-based Z-scheme type photocatalysts for effective tartrazine degradation, Chem. Eng. J. 473 (2023), https://doi.org/10.1016/j.cej.2023.145239.

[47] H. Gupta, S. Chakrabarti, S. Mothkuri, B. Padya, T.N. Rao, P.K. Jain, High performance supercapacitor based on 2D-MoS2 nanostructures, Mater. Today Proc. 26 (2018) 20–24, https://doi.org/10.1016/j.matpr.2019.04.198.

[48] D. Sahoo, B. Kumar, J. Sinha, S. Ghosh, S.S. Roy, B. Kaviraj, Cost effective liquid phase exfoliation of MoS2 nanosheets and photocatalytic activity for wastewater treatment enforced by visible light, Sci. Rep. 10 (2020) 1–12, https://doi.org/10.1038/s41598-020-67683-2.

[49] S.A. Mathew, P. Praveena, S. Dhanavel, R. Manikandan, S. Senthilkumar, A. Stephen, Luminescent chitosan/carbon dots as an effective nano-drug carrier for neurodegenerative diseases, RSC Adv. 10 (2020) 24386–24396, https://doi.org/10.1039/d0ra04599c.

[50] A. Dager, T. Uchida, T. Maekawa, M. Tachibana, Synthesis and characterization of Mono-disperse Carbon Quantum Dots from Fennel Seeds: Photoluminescence analysis using Machine Learning, Sci. Rep. 9 (2019) 1–10, https://doi.org/10.1038/s41598-019-50397-5.

[51] K.C. Lalithambika, K. Shanmugapriya, S. Sriram, Photocatalytic activity of MoS2 nanoparticles: an experimental and DFT analysis, Appl. Phys. A Mater. Sci. Process. 125 (2019) 1–8, https://doi.org/10.1007/s00339-019-3120-9.

[52] A.B.D. Nandiyanto, R. Oktiani, R. Ragadhita, How to read and interpret ftir spectroscope of organic material, Indones, J. Sci. Technol. 4 (2019) 97–118, https://doi.org/10.17509/ijost.v4i1.15806.

[53] S. Han, K. Liu, L. Hu, F. Teng, P. Yu, Y. Zhu, Superior Adsorption and Regenerable Dye Adsorbent Based on Flower-Like Molybdenum Disulfide Nanostructure, Sci. Rep. 7 (2017) 1–11, https://doi.org/10.1038/srep43599.

[54] N. Thomas, S. Mathew, K.M. Nair, K. O'Dowd, P. Forouzandeh, A. Goswami, G. McGranaghan, S.C. Pillai, 2D MoS2: structure, mechanisms, and photocatalytic applications, Mater. Today Sustain. 13 (2021), https://doi.org/10.1016/j.mtsust.2021.100073.

[55] K. Hareesh, A review on carbon quantum dot/semiconductor-based nanocomposites as hydrogen production photocatalysts, RSC Adv. 14 (2024) 23404–23422, https://doi.org/10.1039/d4ra04149f.

[56] A. Taffelli, S. Dirè, A. Quaranta, L. Pancheri, Mos2 based photodetectors: A review, Sensors 21 (2021), https://doi.org/10.3390/s21082758.

[57] P. Sahatiya, S.S. Jones, S. Badhulika, 2D MoS2–carbon quantum dot hybrid based large area, flexible UV–vis–NIR photodetector on paper substrate, Appl. Mater. Today 10 (2018) 106–114, https://doi.org/10.1016/j.apmt.2017.12.013.